Serum BRD2 autoantibody in hepatocellular carcinoma and its detection using mimotope peptide-conjugated BSA

CHANG-KYU HEO[1*], WON-HEE LIM[1,2*], INSEO PARK[1], YON-SIK CHOI[3], KOOK-JIN LIM[3] and EUN-WIE CHO[1,2]

[1]Rare Disease Research Center, Korea Research Institute of Bioscience and Biotechnology;
[2]Department of Functional Genomics, University of Science and Technology, Daejeon 34141;
[3]ProteomeTech Inc., Seoul 07528, Republic of Korea

Received April 21, 2022; Accepted October 10, 2022

DOI: 10.3892/ijo.2022.5448

Abstract. Tumor-associated (TA) autoantibodies are considered to be promising biomarkers for the early detection of cancer, prior to the development of clinical symptoms. In the present study, a novel TA autoantibody was detected, which may prove to be useful as a diagnostic marker of human HCC using an HBx-transgenic (HBx-tg) hepatocellular carcinoma (HCC) mouse model. Its target antigen was identified as the bromodomain-containing protein 2 (BRD2), a transcriptional regulator that plays a pivotal role in the transcriptional control of diverse genes. BRD2 was upregulated in HCC tissues of the H-ras12V-tg mouse and human subjects, as demonstrated using western blotting or immunohistochemical analysis, with the BRD2 autoantibody. In addition, the truncated BRD2 reactive to the BRD2 autoantibody was detected in tumor cell-derived exosomes, which possibly activated TA immune responses and the generation of autoantibodies. For the detection of the serum BRD2 autoantibody, epitope mimicries of autoantigenic BRD2 were screened from a random cyclic peptide CX_7C library with the BRD2 autoantibody. A mimotope with the sequence of CTSVFLPHC, which was cyclized by one pair of cysteine residues, exhibited high affinity to the BRD2 autoantibody and competitively inhibited the binding of the autoantibody to the cellular BRD2 antigen. The use of this cyclic peptide as a capture antigen in human serum enzyme-linked immunosorbent assay allowed the distinction of patients with HCC from healthy subjects with 64.41% sensitivity and 82.42% specificity (area under the ROC curve, 0.7761), which is superior to serum alpha-fetoprotein (AFP; 35.83% sensitivity; 100% specificity; area under the ROC curve, 0.5337) for the diagnosis of HCC. In addition, the detection of the BRD2 autoantibody combined with other autoantibody biomarkers or AFP has increased the accuracy of HCC diagnosis, suggesting that the combinational detection of cancer biomarkers, including the BRD2 autoantibody, is a promising assay for HCC diagnosis.

Correspondence to: Dr Eun-Wie Cho, Rare Disease Research Center, Korea Research Institute of Bioscience and Biotechnology, 125 Gwahak-ro, Yuseong-gu, Daejeon 34141, Republic of Korea
E-mail: ewcho@kribb.re.kr

*Contributed equally

Key words: autoantibody biomarker, bromodomain-containing protein 2, hepatocellular carcinoma, cyclic peptide mimotope, human serum ELISA

Introduction

Cancer is one of the leading causes of mortality worldwide, as it accounted for almost 10 million deaths in 2020, or nearly one in six deaths, with the most common cancers being breast, lung, colon and rectum and prostate cancers (1). Primary liver cancer is also a challenging global health concern, as more than one million individuals are estimated to be affected annually by the year 2025. The most common type of liver cancer is hepatocellular carcinoma (HCC), the incidence of which has been increasing worldwide, mostly due to chronic viral hepatitis B infection (2). Recently, non-alcohol-related steatohepatitis has also rapidly emerged as another etiological concern (3,4).

In common clinical practice, HCC is diagnosed using non-invasive criteria, including a serum alpha-fetoprotein (AFP) or ultrasound test, and the treatment applied may vary, depending on the overall tumor burden and underlying liver disease severity (2). However, novel evidence points towards the importance of histology and of the characterization of the molecules that drive pathogenesis, to identify druggable targets (5,6). Moreover, immunotherapies that instigate the host immunity to induce a systemic response against tumors currently offer much clinical promise (7). Therefore, the clinical classification of HCC using appropriate biomarkers accompanied by treatment is important for the improvement of of the prognosis of patients with HCC.

The majority of malignant tumors can be recognized by the host immune-surveillance defensive system, namely, natural killer (NK) and T-cells; however, cancer cells evolve to acquire genetic instabilities and other associated 'hallmarks' that can enable persistent growth and immune evasion from NK or T-cells, in spite of their presence near tumors (8). Unlike T-cells, relatively few B-cells are found in tumor infiltrates and have been rarely studied. However, their existence and

functionality have been recently suggested as important prognostic factors for the response to immunotherapy (9). Furthermore, the plasma cells present in tumor infiltrates produce large amounts of cytokines and tumor-associated (TA) antibodies, even with reduced cell counts, and these soluble factors can serve as significant biomarkers (9).

TA antibodies have been examined in patients with cancer for several decades. The levels of serum autoantibodies against TA self-antigens have been proposed as early markers of cancer (10-12). Moreover, serum autoantibodies can serve as potent prognostic markers at later stages of disease (13), which may be related to the prognostic significance of tumor-infiltrating B-cells (14,15). Therefore, screening significant autoantibody biomarkers related to cancer and identifying appropriate combined therapies may be necessary for precision cancer medicine in the future.

In the present study, a bromodomain-containing protein 2 (BRD2) autoantibody was reported as a novel TA autoantibody biomarker for HCC. B-cell hybridoma pool obtained from the HBx-transgenic HCC tumor-bearing mouse model (16-18) was screened using human liver cancer cells, and one TA autoantibody, XC246, was obtained. Using the purified XC246 autoantibody, its target antigen was identified as BRD2, a transcriptional regulator of diverse genes, and the neo-antigenic properties of BRD2 in liver cancer cells were analyzed. The present study also screened the mimicries of the epitope on the autoantigen BRD2 from a random cyclic peptide library and used it to develop a serum autoantibody enzyme-linked immunosorbent assay (ELISA). Finally, the significance of the BRD2 autoantibody as a cancer diagnostic marker was evaluated using cyclic peptide ELISA and compared with other serum biomarkers.

Materials and methods

HCC-associated autoantibody. A monoclonal TA autoantibody, XC246, was prepared from a B-cell hybridoma generated from the splenocytes of HBx-transgenic mice bearing HCC tumors (18). The isotype of the XC246 autoantibody was determined as IgM using an isotyping kit (Thermo Fisher Scientific, Inc.). The XC246 autoantibody was purified from hybridoma-cell culture media using protein L agarose (Thermo Fisher Scientific, Inc.) and applied in further studies after analysis, using SDS-PAGE and western blotting.

Cell lines. The following human cancer cell lines were obtained from the American Type Culture Collection (ATCC) or the Korean Cell Line Bank (KCLB): The liver cancer cells, HepG2 (ATCC HB-8065), Hep3B (ATCC HB-8064), PLC/PRF/5 (ATCC CRL-8024), Huh7 (KCLB 60104) and SK-HEP1 (ATCC HTB-52); the gastric cancer cells, SNU638 (KCLB 00638); the lung cancer cells, A549 (ATCC CRM-CCL-185); the colorectal cancer cells, HT-29 (ATCC HTB-38); the prostate cancer cells, LNCaP/LN3 (KCLB 80018); the cervical cancer cells, HeLa (ATCC CRM-CCL-2); and the breast cancer cells, SK-BR-3 (ATCC HTB-30). The cells were cultured in Dulbecco's modified Eagle's medium (DMEM) or RPMI-1640 (Invitrogen; Thermo Fisher Scientific, Inc.) supplemented with 10% inactivated fetal bovine serum (FBS; Sigma-Aldrich). Conditioned media containing exosomes were prepared from 70 to 80% confluent HepG2 cells, which were cultured in complete DMEM for 48 h with 10% exosome-free FBS (System Biosciences, LLC). The cell lines (HepG2, HT-29 and SK-HEP1) were authenticated using short tandem repeat (STR) analysis by the Korean Cell Line Bank (KCLB), and the STR profile results are presented in Data S1.

The expression of recombinant human BRD2 in E. coli. For the expression of full-length and a series of truncated BRD2 proteins (hBRD2: NM_005104.4) with N-terminal 3xFLAG-tag [(DYKDDDDK)x3] were cloned into the pE28a(+) vector (Novagen, Sigma-Aldrich) using *Nde*I and *Xho*I. Expression vectors were transformed into *E. coli* strain SHuffle® T7 (New England Biolabs, cat. no. C3029J). The *E. coli* SHuffle® T7 transformants were grown at 30˚C for 16 h in 2xYT broth (16 g Bacto Tryptone, 10 g Bacto Yeast Extract, 5 g sodium chloride in 1 l distilled water, pH 7.0) containing kanamycin (50 μg/ml). The culture was diluted 100-fold into fresh 2xYT medium and grown in a shaking incubator at 30˚C. When the OD600 of the cultures reached 2.0, isopropyl-β-D-thiogalactopyranoside (IPTG; Sigma-Aldrich cat. no. 16758) was added to a final concentration of 1 mM and incubation was continued at 25˚C for 22 h. Cells were harvested by centrifugation at 3,000 x g for 30 min at 4˚C. The cell pellets were solubilized in 5X SDS-PAGE sample buffer and used for further analysis.

SDS-PAGE and western blot analysis. The purified antibody or epitope-conjugated bovine serum albumin (BSA) was analyzed by using 10% SDS-PAGE and Coomassie brilliant blue staining. Western blot analysis of cell or tissue lysates was performed as previously described (18). Total cell or tissue lysates were prepared in radioimmunoprecipitation assay (RIPA) buffer containing a protease inhibitor cocktail (Sigma-Aldrich). The liver tissues from the H-ras mice were already available as part of a previous study (18). For subcellular fractionation, cells were lysed using NE-PER™ Nuclear and Cytoplasmic Extraction Reagents kit (Thermo Fisher Scientific, Inc. cat. no 78833). Exosomes were collected from the conditioned media using an exosome isolation kit ExoQuick-TC (System Biosciences, LLC, cat. no. EXOTC50A-1) or by ultracentrifugation at 100,000 x g for 1 h at 4˚C, and lysed in RIPA buffer (17). The protein concentration was determined using Bradford reagent (Bio-Rad Laboratories, Inc.). Equal amounts of protein (10 μg per lane) were analyzed using western blotting with the indicated primary antibodies. Briefly, proteins were separated by 12% sodium dodecyl sulfate-polyacrylamide gel electrophoresis (SDS-PAGE), and transferred onto PVDF membranes (MERCK, cat. no. IPVH00010). After blocking with 5% BSA in Tris-buffered saline with 0.1% Tween-20 (TBST) at 25˚C for 60 min, the membranes were probed with primary antibodies at 25˚C for 2 h. After washing with TBST, the membranes were probed with HRP-conjugated secondary antibodies. The membranes were then washed with TBST and antigens were detected with enhanced chemiluminescence reagent (MERCK, cat. no. GERPN2106). β-actin or GAPDH was probed as loading controls. The primary antibodies used in this study were as follows: BRD2 (Novus Biologicals, cat. no. NBP1-84310, NBP1-30475; 1:1,000 dilution), AICAR transformylase/inosine monophosphate cyclohydrolase (ATIC;

Thermo Fisher Scientific, cat. no. MA1-086; 1:500 dilution), programmed cell death 6-interacting protein (ALIX; exosomal marker; Merck Millipore, cat. no. ABC1435; 1:500 dilution), calnexin (endoplasmic reticulum marker; Santa Cruz Biotechnology, cat. no. sc-46669; 1:1,000 dilution), GAPDH (Santa Cruz Biotechnology, cat. no. sc-47724; 1:5,000 dilution), and β-actin (Santa Cruz Biotechnology, cat. no. sc-8432; 1:5,000 dilution). Anti-mouse IgG-horseradish peroxidase (HRP; Cell Signaling Technology, cat. no. #7076S; 1:2,500 dilution) or anti-rabbit IgG-HRP (Cell Signaling Technology, Inc. cat. no. 7074S; 1:2,500 dilution) were used as secondary antibodies. Band intensities were quantified using ImageJ v1.52a (National Institutes of Health), and the relative intensity compared with that of β-actin or GAPDH was calculated. For the immunoprecipitation analysis of the XC246 antigen, 600 μg of HepG2 cell lysate was incubated with XC246 antibody-conjugated agarose beads (bead volume, 20 μl) for 16 h at 4˚C; after a brief washing the beads in RIPA buffer by centrifugation at 1,000 x g for 30 sec at 4˚C, the agarose beads were analyzed by western blotting. For the proteomics analysis of the XC246 antigen, 500 μl of antibody-conjugated beads was used for immunoprecipitation with 9.69 mg of SNU638 cell lysate. As a control, blank agarose beads without the immobilized antibody were used. XC246 antibody-conjugated agarose beads were prepared using a co-immunoprecipitation kit (Thermo Fisher Scientific, cat. no. 26149). For competitive western blot analysis, 5 μg of the XC246 primary antibody in 10 ml of 5% skim milk in TBS was pre-incubated with epitope-peptide-conjugated BSA (2 μg) at 25˚C for 90 min and then used as the primary antibody for probing the blot.

Flow cytometric analysis. Cells were fixed and permeabilized with BD Cytofix/Cytoperm solution (BD Biosciences) at 4˚C for 30 min. The cells were then incubated with the XC246 primary antibody solution and secondary reagent goat anti-mouse IgG F(ab')2-PE (Thermo Fisher Scientific, cat no. A10543; 1:400 dilution) at 4˚C for 40 min. The stained cells were analyzed on a FACSCalibur (BD Biosciences) instrument, and the obtained data were analyzed using the CellQuest software v6.0 (BD Biosciences). When determining whether the autoantibody-mimotope display phages could compete with the target cellular antigen for antibody binding, the XC246 primary antibody was pre-incubated with each mimotope-display phage at 25˚C for 60 min and then used as primary antibody solution.

Immunofluorescence. Cells were plated on glass coverslips and, after an additional 48 h, were used for immunofluorescence detection, as described previously (17). Cells were fixed and permeabilized with BD Cytofix/Cytoperm solution (BD Biosciences), washed with BD Cytoperm/wash solution (BD Biosciences), and incubated with the primary antibody in wash-solution (5 μg/ml) at 4˚C for 16 h. After washing with wash-solution, the cells were treated with goat anti-mouse IgGAM-rhodamine (Abcam, cat. no. ab6004) or anti-rabbit IgG-FITC (Abcam, cat. no. ab6798) in wash-solution (1:1,000 dilution) at 25˚C for 1 h, followed by mounting on a DAPI-containing mounting medium (Vector Laboratories, cat. no. H-1200). Confocal microscopic analysis was performed using a Zeiss LSM 510 Meta microscope (Zeiss AG). The staining with an anti-FBXO2 antibody (mouse IgM; Santa Cruz Biotechnology, cat. no. sc-393873) was performed under the conditions described above to confirm the accessibility of the IgM antibody to the nucleus.

Immunohistochemistry (IHC). A paraffin-embedded human HCC BioMax Array (cat. no. LV1201b) was purchased from US BioMax Inc. Biopsy features included age, sex, organ or anatomic site involved, grading and pathological diagnosis (H&E-stained sections). The HCC tissue array was comprised of HCC or HCC-related liver disease tissues and normal liver tissues as follows: i) 10 cases of benign tumor (cavernous hemangioma); ii) 14 cases of normal liver tissues; iii) 25 cases of hepatocellular carcinoma (stage I, n=1; stage II, n=16; stage III, n=5; stage IV, n=3); iv) 29 cases of cirrhosis; v) 22 cases of chronic hepatitis; and vi) 13 cases of fatty degeneration. US Biomax states that 'All tissue is collected under the highest ethical standards with the donor being informed completely and with their consent. We make sure we follow standard medical care and protect the donors' privacy. All human tissues are collected under HIPPA approved protocols. All animal tissues are collected under IACUC protocol. All samples have been tested negative for HIV and hepatitis B or their counterparts in animals, and approved for commercial product development'. The Public Institutional Review Board of the Ministry of Health and Welfare reviewed the contents of the present study and confirmed that research using commercialized human tissue falls under the exemption categories specified by Bioethics and Safety Act in Korea (IRB, approval no.: P01-202008-31-009; Republic of Korea). The immunohistochemical staining for XC246 antigen was performed using XC246 monoclonal autoantibody (2 μg/ml) as previously described (16). The IHC staining of all tissues was performed under identical conditions, as tissues with all pathological characteristics were present on one slide. The endogenous peroxidase activity was blocked by treatment with 4% H_2O_2/methanol for 10 min, and this was followed by remaining staining protocol. The photomicrographs were acquired at x200 or x400 magnification using a multi-view fluorescence microscope (BX51; Olympus Corporation). The DAB intensity of each staining using DAB kit (GBI Labs, cat. no. D22-6) was quantified by ImageJ v1.52i software (National Institutes of Health) and plotted.

Mass spectrometry (MS) analysis of the XC246 antigen. For the enrichment of the antigen against the XC246 autoantibody, a SNU638 cell lysate prepared with RIPA cell lysis buffer was immunoprecipitated using XC246 antibody-conjugated beads as described above. Subsequently, the beads were treated with 0.1 M glycine buffer (pH 2.5) to elute the target antigen, and the eluate was neutralized with 1.0 M Tris buffer (pH 8.0). The eluates were then separated using 10% SDS-PAGE, followed by western blotting or Coomassie brilliant blue staining at 25˚C for 2 h. The Coomassie-stained band corresponding to the XC246 antigen band was confirmed using western blotting. The XC246 antigen band was then excised and in-gel digested with trypsin (Promega Corporation). Protein identification was performed via ESI-TRAP mass spectrometry (LTQ Orbitrap XL Hybrid Ion Trap Mass Spectrometer; Thermo Fisher

Scientific, Inc.) and Mascot database search at the Korea Basic Science Institute (Ochang, Korea).

Knockdown of candidate antigens and reverse transcription polymerase chain reaction (RT-PCR). To verify whether the candidate proteins identified by mass spectrometric analysis corresponded to the XC246 antigen, the HepG2 cells were transfected with siRNAs, targeting the candidate genes (Bioneer Corporation and Thermo Fisher Scientific Inc.) using Lipofectamine RNAimax reagent (Thermo Fisher Scientific Inc.), followed by western blot analysis using the XC246 antibody. The sequences of the siRNAs were as follows: siRNA for the elongation factor 2 (si-EEF2) si-sense, 5'-GAGAUGUAU GUGGCCAAGUtt-3' and antisense, 5'-ACUUGGCCACAU ACAUCUCtt-3'; siRNA for the isoform 3 of unconventional myosin 1c (si-MYO1C) sense, 5'-GACCAAGACAGCCCU CAGUtt-3' and antisense, 5'-ACUGAGGGCUGUCUUGGU Ctt-3'; si-BRD2 sense, 5'-CUGGGAGUCUUGAGCCUA Att-3' and antisense, 5'-UUAGGCUCAAGACUCCCAGga-3'; si-control sense, CCUACGCCACCAAUUUCGU(dTdT) and antisense, ACGAAAUUGGUGGCGUAGG(dTdT). The siRNA-treated cells were analyzed 72 h after transfection. RT-PCR was performed using primer pairs purchased from Bioneer Corporation, as follows: EEF2 sense, 5'-GTGGAG AACGTGAACGTCATC-3' and antisense, 5'-GAAGGTGCG TGGCAGCTTCT-3'; MYO1C sense, 5'-CGCTACCGGGCG TCGGCC-3' and antisense, 5'-CGTGCGCAGTGCTCGGT AC-3'; BRD2 sense, 5'-AGAGTCCTCCAGTGAGGAAAG-3' and antisense, 5'-CCACTGCCACTTGCTTTCTTG-3'. GAPDH sense, 5'-CCAATATGATTCCACCCATGGC-3' and antisense, 5'-GCTGATGATCTTGAGGCTGTTG-3'. Briefly, total RNA was extracted from the siRNA transfectants using the RNeasy Plus mini kit (Qiagen, Germany, cat. no. 74134) following the manufacturer's protocol. Reverse transcription (RT) was performed using the GoScript™ Reverse Transcription Mix kit (Promega Corporation, cat. no. A2791). PCR was carried out using 2X Taq PCR Pre-Mix (BIOFACT, cat. no. ST302-10h) using a Verti 96 well Thermal Cycler (Invitrogen; Thermo Fisher Scientific, Inc.) which was performed by an initial denaturing step at 95˚C for 5 min followed by 27 cycles of denaturation at 95˚C for 10 sec, 55-62˚C for 30 sec for annealing and elongation at 72˚C for 30 sec. At the end of additional elongation at 72˚C for 5 min, PCR products were analyzed by 1% agarose gel electrophoresis. The relative levels of each PCR product were quantified using ImageJ v1.53k software and normalized to that of GAPDH.

Biopanning of the XC246-specific cyclic peptide mimotopes. For the selection of the mimotope specific to XC246 autoantibody, the phage-display random cyclic peptide library Ph.D.™-CX_7C (New England Biolabs, Inc.) was used, as previously described (16-18). Panning was repeated four times, and the mimotope sequences were determined by sequencing the selected phages according to the manufacturer's instructions. DNA sequencing was performed by Bioneer Corporation based on Sanger method using -96gIII sequencing primer (5'-CCCTCATAGTTAGCGTAACG-3').

ELISA. ELISA was performed as previously described, with some modifications (17). Briefly, ELISA plates (Nunc Maxisorp; Thermo Fisher Scientific, Inc.) were coated with the indicated amount of antigen [cyclic peptide epitope-display M13 phages or epitope-miniPEG2-conjugated BSA] in PBS (pH 7.4) overnight at 4˚C and blocked with Protein-Free Blocking Buffer (PFBB; Thermo Fisher Scientific, Inc.). The CX_7C peptide mimotopes were synthesized and cyclized via terminal cysteine residues. The cyclized peptides were then coupled to miniPEG2 spacer via the free amine residue at the amino terminus of the peptide. The PEG-conjugated cyclic peptides were synthesized and purified by Peptron. Cyclic peptide-miniPEG2-conjugated BSA was prepared using the EDC coupling method (Thermo Fisher Scientific, Inc.). The miniPEG2-conjugated BSA without the peptide epitope was used as the control antigen. The primary antibody or secondary reagent solution was prepared in PFBB. Anti-mouse IgGAM-HRP (Thermo Fisher Scientific, Inc.) was used as the secondary reagent. To detect the human autoantibody in patients' sera, ELISA plates were coated with XC246p9-miniPEG-conjugated BSA at 500 ng/well. After blocking with a buffer containing 1% polyvinyl alcohol (molecular weight, 14-15k; MilliporeSigma) and 1% Ficoll P400 (MilliporeSigma) in TBS, the plates were treated with human sera (1:50 dilution in blocking buffer) at 37˚C for 90 min and detected using HRP-conjugated anti-human IgGAM antibody (Thermo Fisher Scientific, Inc.; 1:2,000 dilution). Serum AFP was quantified using a human alpha-Fetoprotein Quantikine ELISA kit (R&D Systems, cat. no. DAFP00). The present study using human HCC and normal serum samples was conducted after receiving an exemption from the Public Institutional Review Board of the Ministry of Health and Welfare (IRB No.: P01-202008-31-009; Republic of Korea). Human serum samples were obtained from the National Biobank of Korea, which is supported by the Ministry of Health and Welfare. Serum samples were kept at -80˚C until further use.

Statistical analysis. All data are presented as the mean ± standard deviation (SD) and were analyzed using a two-tailed unpaired Student's t-test or one-way ANOVA followed by the Bonferroni post-hoc test. The results of ELISA were evaluated using receiver operating characteristics (ROC) analysis, leading to estimates of the area under the ROC curve (AUC), with 95% confidence intervals (CIs). The correlation between the biomarkers was assessed using Pearson's correlation analysis. Statistical analyses were performed using the Prism 7 software (GraphPad Software, Inc.). $P<0.05$ was considered to indicate a statistically significant difference.

Results

The TA autoantibody XC246 identified in the HBx-tg HCC mouse model displays an increase in target antigen expression in human HCC tissues. HBx-transgenic mice, which exhibit spontaneous generation of liver cancer at 10-13 months after birth, have been proven to be suitable for the study of human HCC (19-21). Previously, three HCC-associated autoantibodies were identified by the authors using B-cell hybridoma cells constructed using tumor-bearing HBx-transgenic mice (16-18). In the present study, a monoclonal TA autoantibody, which was termed XC246, was identified, and its antigenic characteristics were analyzed. Firstly, the presence of an antigen reactive to

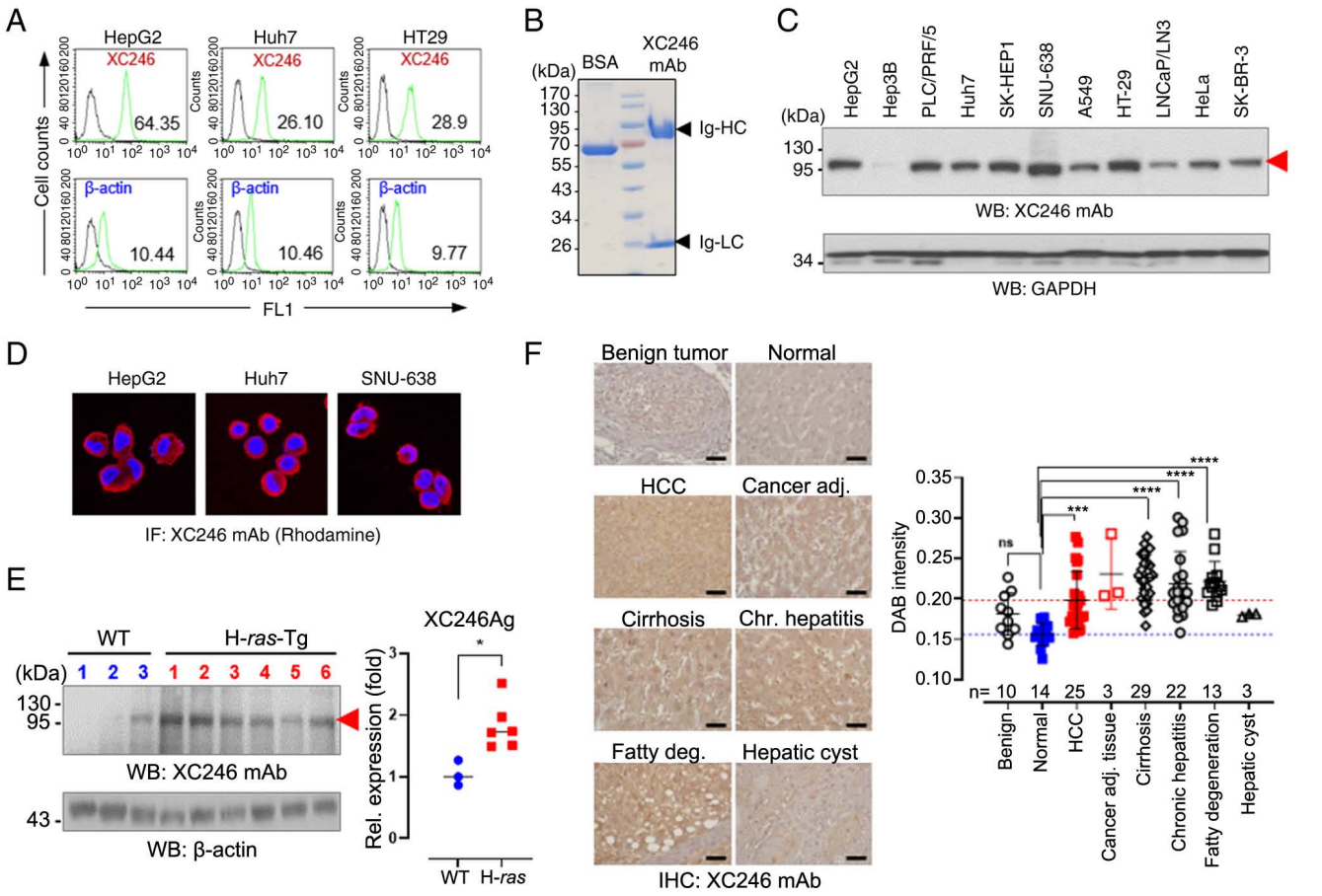

Figure 1. The tumor-associated monoclonal autoantibody, XC246, was identified in the HBx-Tg HCC mouse model. (A) Flow cytometric analysis of intracellular stained tumor cell lines with the XC246 autoantibody. Fixed and permeabilized cells were treated with XC246 hybridoma-cultured media, followed by staining with PE-labeled anti-mouse IgG. β-Actin staining was also performed, and the relative ratio of XC246 to β-actin staining was plotted. (B) SDS-PAGE analysis of purified XC246 monoclonal autoantibody. Purified XC246 antibody (5 μg) was treated with reducing SDS-PAGE sample buffer and separated on 10% SDS-PAGE. The Coomassie blue-stained gel revealed the immunoglobulin μ heavy chain with a molecular weight of 72 kDa and the light chain with a molecular weight of 25 kDa. BSA (5 μg) was loaded as a control. (C) Western blot analysis of XC246 antigen expression in various human tumor cell lines (cell lysates; 10 μg per lane). GAPDH served as an internal control. The red arrow indicates the XC246 antigen. (D) Immunofluorescence staining of the XC246 antigen in human cancer cells (human liver cancer cell lines HepG2 and Huh7; gastric cancer cell line SNU638). Fixed and permeabilized cells were treated with purified XC246 antibody, followed by staining with Rhodamine-labeled anti-mouse IgG antibody. (E) Expression of XC246 Ag in liver tissues of H-ras12V-tg mice. The liver tissue lysates (50 μg) of wild-type mice (n=3) or tumor-bearing H-ras12V-tg mice (n=6) were separated on 10% SDS-PAGE, and western blots were probed with the XC246 autoantibody. Band intensities were quantified using ImageJ software, and the values were normalized to those of β-actin. (F) IHC of a human liver tissue microarray. A tissue microarray containing benign tumor (liver hemangioma; n=10), normal (n=14), HCC (n=25), cirrhosis (n=29), chronic hepatitis (n=22), or fatty liver (n=13) tissues was stained with the XC246 antibody (0.5 μg/ml). Representative images of IHC staining are presented. H&E stains are included in Fig. S1. Scale bar, 50 μm. The DAB intensities of IHC images were quantified using ImageJ software, and the quantified values were plotted. Statistical significance was determined using (E) a two-tailed Student's t-test or (F) one-way ANOVA followed by the Bonferroni post-hoc test. *P<0.05, ***P<0.001 and ****P<0.0001. ns, not significant (P>0.05); HCC, hepatocellular carcinoma; BSA, bovine serum albumin; IHC, immunohistochemistry.

the XC246 autoantibody in human cancer cells was examined using flow cytometry. For the staining of intracellular antigens, cells were fixed and mildly permeabilized with a paraformaldehyde/saponin solution, to maintain the conformational epitopes on the target antigens. The XC246 TA autoantibody in hybridoma-cultured media reacted to human liver cancer cells, including HepG2 and Huh7 cells (Fig. 1A). The colorectal cancer HT-29 cells also exhibited reactivity to the XC246 autoantibody. These results indicated that TA autoantigen against XC246 TA autoantibody generated in a mouse HCC tumor model may also be expressed in human tumor cell lines. The isotype of the XC246 antibody was determined using an isotyping kit as being IgM with a kappa light chain (data not shown). For the identification and characterization of the target antigen of the XC246 TA autoantibody, the antibody was purified from hybridoma-cultured media using protein L agarose. SDS-PAGE analysis of the purified antibody showed the presence of IgM heavy and light chains (Fig. 1B).

The target antigen of XC246 antibody was analyzed by western blot analysis of human tumor cell lines. As depicted in Fig. 1C, the XC246 antibody reacted to a specific antigen (termed XC246 Ag) with a molecular weight of about 110 kDa. XC246 Ag was ubiquitously and highly expressed in various human tumor cells, including liver cancer (HepG2), gastric cancer (SNU638) and colorectal cancer (HT-29); however, its expression was unusually low in Hep3B cells. XC246 Ag was noted to be mainly localized to the cytoplasm, as demonstrated by tumor cell immunofluorescence staining (Fig. 1D). Of note, XC246 antibody detected a target antigen of ~110 kDa in liver tumor tissues of H-ras12V transgenic mice (Fig. 1E).

The same antigen was also detected in non-transgenic mice; however, its expression was lower than that in tumor tissues ($P \leq 0.05$; Fig. 1E), which implies that the upregulation of the XC246 antigen is associated with tumorigenesis. XC246 antigen expression was also higher in human HCC tissues than in normal liver tissues, as shown by immunohistochemical staining ($P \leq 0.001$; Figs. 1F and S1). Of note, its expression was significantly increased in patients with chronic hepatic liver diseases ($P \leq 0.0001$), including cirrhosis and chronic hepatitis.

Overall, these results suggested that the HCC-associated autoantibody XC246 may react with a specific antigen expressed in the cytoplasm of human or mouse tumor cells with a molecular weight of ~110 kDa and that its expression was increased in HCC and chronic liver diseases.

The target antigen of the TA autoantibody XC246 is BRD2, a transcriptional regulator secreted from tumor cells as an exosomal component. The target antigen of the XC246 autoantibody was identified using MS analysis. The lysate of SNU638 cells was immunoprecipitated using XC246 antibody-conjugated agarose beads, and its eluate was separated on preparative 10% SDS-PAGE. As a control, the immunoprecipitates using agarose beads without antibodies were used. A tenth of the immunoprecipitates was analyzed using western blot analysis, revealing that the XC246 antigen was enriched in the immunoprecipitated fraction (Fig. 2A). The protein band on the preparative SDS-PAGE that corresponded to the immuno-stained antigen was then excised, in-gel digested and analyzed via ESI-TRAP MS (Fig. 2A). The isoelectric point (pI) of the XC246 antigen was also examined by two-dimensional gel electrophoresis of a total HepG2 cell lysate, followed by western blot analysos using the XC246 antibody; the pI of the 110-kDa antigen was estimated to be ~9 (Fig. S2). The identified proteins in MS analysis that exhibited a high %mol/score are listed in Table I.

Based on the protein data acquired, including molecular weight and pI, three candidate proteins (EEF2, BRD2 and MYO1C) were selected for further validation. The downregulation of the XC246 antigen following the knockdown of each candidate gene was examined. The knockdown of BRD2 in HepG2 cells clearly reduced the expression of the XC246 antigen, as demonstrated using western blot analysis with the XC246 antibody. By contrast, the knockdown of the remaining candidates (EEF2 or MYO1C) had no or only a minimal effect on XC246 antigen levels (Fig. 2B). BRD2 was also confirmed as the XC246 antigen by analysis of the immunoprecipitates obtained with the XC246 antibody (Fig. 2C). The commercial anti-BRD2 antibody detected the target antigen with a molecular weight of ~110 kDa in cell lysate input or flow-through fractions. It also detected the immunoprecipitates obtained with the XC246 antibody, the molecular weight of which was identical to that of the BRD2 protein. Collectively, these results confirmed that the XC246 antigen, which induced the expression of the TA autoantibody in the HCC mouse model, was BRD2.

The BRD2 gene encodes a transcriptional regulator that belongs to the bromodomain and extra-terminal domain (BET) family of proteins. BRD2 associates with transcription complexes and acetylated chromatin during mitosis; it then selectively binds to the acetylated lysine 12 residue of histone H4 via its two bromodomains (22). Decreased BRD2 expression has been associated with longevity-promoting processes (23,24), whereas increased BRD2 expression can promote cancer in murine hematopoietic cells and B lymphocytes (25). The Cancer Genome Atlas (TCGA) has demonstrated that BRD2 expression is elevated across 32 distinct tumor types and established BRD2 as a promising drug target for human cancers (26). The downregulation of BRD2 in HeLa cells leads to a 60% increase in tumor-suppressing p53 levels (27), which also supports the notion that increased BRD2 promotes cancer growth. Hence, the overexpression of BRD2 in HCC can be oncogenic, whereas the inhibition of the activity of BRD2 limits cancer progression. More importantly, Kaplan-Meier analysis of overall survival in patients with HCC by their BRD2 protein expression levels revealed BRD2 as a poor prognostic marker for liver cancer (Fig. S3). The mouse BRD2 protein (NP_001191902) presents with 96% amino acid sequence identity (97% similarity) to human BRD2 (NP_005095), which is composed of 801 amino acids. The difference between the mouse and human BRD2 protein sequences was primarily found between the 590 and 630th amino acids of human BRD2, a linker region located between the nuclear localization signal and the extra-terminal (ET) domain. The sequences of other domains were well conserved (Fig. S4), on which the target sequence of the XC246 antibody may be located.

The protein function of BRD2 mentioned above raised a question about its cellular localization. BRD2 is a transcriptional regulator that functions mainly in the nucleus. However, the XC246 antigen was immunostained with the XC246 antibody mainly in the cytoplasmic region, as demonstrated in Fig. 1D. To examine the cellular localization of the XC246 antigen or BRD2, intracellular staining with a commercial anti-BRD2 antibody or the XC246 autoantibody was performed. The accessibility of XC246 antibody, a mouse pentameric IgM, within the nucleus was confirmed by control staining with an anti-FBXO2 antibody, the isotype of which is IgM. As depicted in Fig. 2D, the commercial anti-BRD2 antibody stained BRD2 mainly within the nucleus. This antibody also stained the cytoplasmic region, although at reduced levels. By contrast, XC246 autoantibody stained the cytoplasmic region mainly (Figs. 1D and 2D). However, the nuclear staining of XC246 is more evident in Fig. 2D compared with Fig. 1D, which may be caused by different staining conditions or image capture settings. The reactivity of XC246 autoantibody to the intracellular fractions was examined again using western blot analysis (Figs. 2E and S5). The XC246 autoantibody stained the 110-kDa antigen with a similar ratio in cytoplasmic or nuclear fractions of HepG2 cells separated on the blot; however, the commercial anti-BRD2 antibody stained cytoplasmic BRD2 at half the strength observed for nuclear BRD2 in the same blot. These results imply that these two antibodies against BRD2 have different epitopes on the BRD2 protein. In addition, the XC246 autoantibody is more reactive to cytoplasmic BRD2, which may possess specific post-translational modifications related to its cytoplasmic localization.

Another important aspect of TA autoantigens is their exposure to immune cells. The increased intracellular antigen must be exposed to the immune cells to induce a specific immune response, ultimately leading to the production

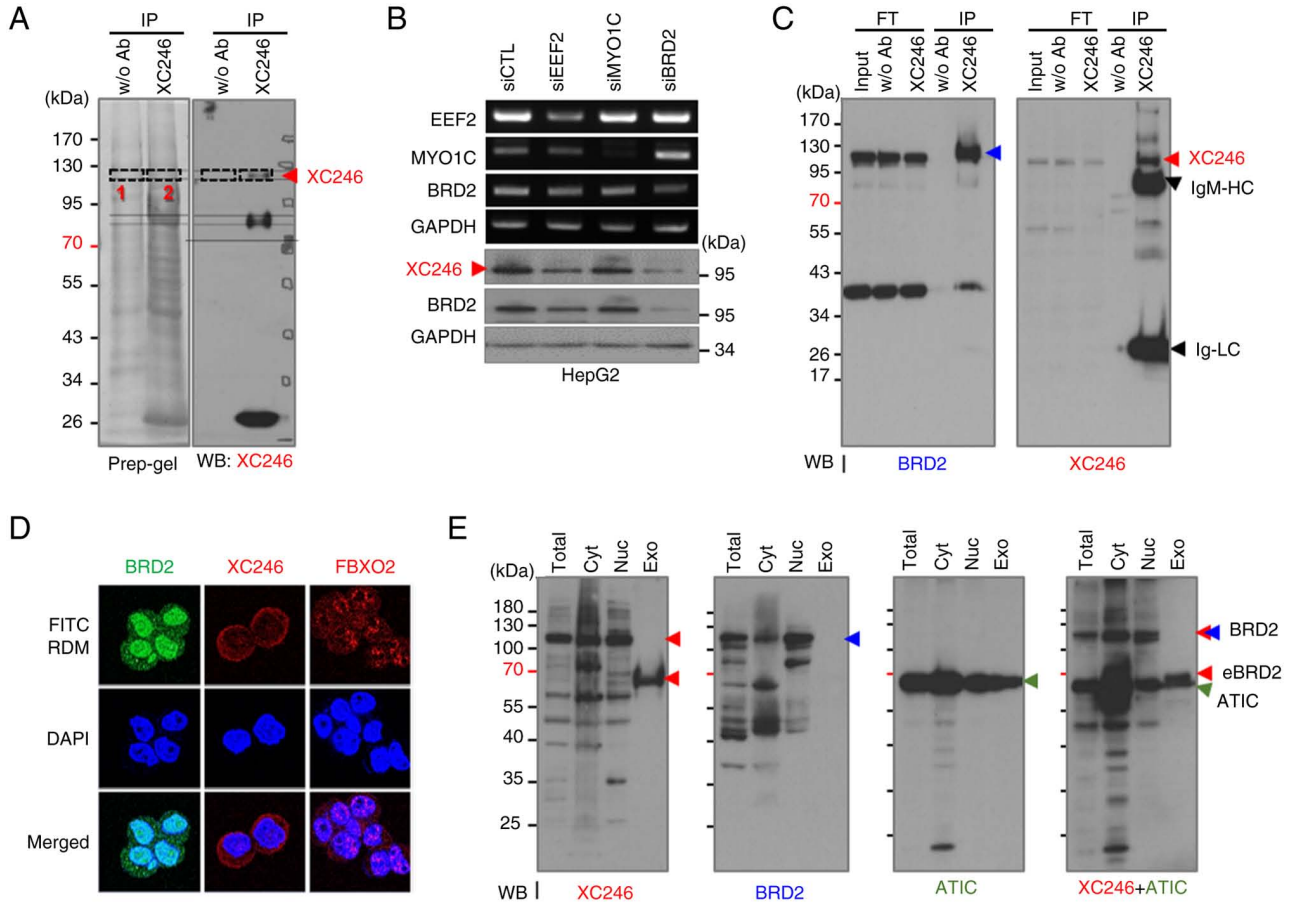

Figure 2. The target antigen of the XC246 autoantibody was identified as BRD2. (A) Preparative 10% SDS-PAGE was performed to isolate the XC246 antigen, and in-gel digestion was carried out for mass spectrometric-based protein identification. A preparative SDS-PAGE gel for western blotting was divided into two sections and blotted separately. The western blotting result is a combined image of two blots, with a dotted line representing the edges of two images. The protein band containing the XC246 antigen confirmed by western blotting was excised (indicated by the red arrow) and in-gel digested with trypsin. The proteins identified by mass spectrometric analysis are listed in Table I. (B) Validation of the XC246 antigen as BRD2 by an RNA interference assay. HepG2 cells were transfected with siRNAs for candidate genes (EEF2, MYO1C and BRD2), and their cell lysates were examined by western blotting with the XC246 antibody. The knockdown of target genes was confirmed using reverse transcription polymerase chain reaction or western blotting. GAPDH was used as an internal control. (C) Immunoprecipitation analysis for the verification of the XC246 antigen as BRD2. The HepG2 cell lysate was immunoprecipitated with XC246 antibody-conjugated agarose beads and analyzed by western blotting with an anti-BRD2 or the XC246 antibody. Immunoprecipitates obtained using agarose beads without antibody conjugation were used as the control. Red arrows indicate the XC246 antigen or BRD2. (D) Immunofluorescence staining of the XC246 antigen in HepG2 cells. Fixed and permeabilized cells were treated with purified XC246 antibody or an anti-BRD2 antibody, followed by staining with FITC- or RDM-labeled anti-mouse IgG. To visualize the nuclei, cells were stained with DAPI. To verify the nuclear permeability of stained cells, an IgM-type mouse antibody (FBXO2 antibody) was also employed. (E) Western blot analysis of the intracellular distribution of the XC246 antigen or BRD2. Total cell lysates, subcellular fractions (cytosolic or nuclear fractions), and exosome lysates were prepared as described in the 'Materials and methods' and analyzed using western blotting. The blots were probed with the XC246 autoantibody, anti-BRD2 antibody, or anti-ATIC antibody. Each target antigen is indicated by colored arrows (red: XC246 and exosome XC246 antigen; blue: BRD2; green: ATIC). BRD2, bromodomain-containing protein 2; RDM, rhodamine; ATIC, AICAR transformylase/inosine monophosphate cyclohydrolase.

of TA autoantibodies. The release of cellular components after cell death or necrosis accompanying tumorigenesis has been assumed to be a mechanism to expose intracellular proteins because most of the TA autoantigens reported to date are intracellular proteins, including p53 (28,29). However, a previous study on TA exosomes revealed that the intracellular components included in exosomes can be exposed to immune cells without cell death (30). In addition, the tumor-derived exosomes can stimulate or suppress immune responses (30,31). As described above, the XC246 antigen appears to be a post-translationally modified BRD2 mainly localized in the cytoplasm. The exosomes secreted by HepG2 cells were examined using western blot analysis to confirm the secretion of BRD2 via exosomes. ATIC (16), another TA autoantigen previously studied, was detected in the exosomes, as shown in Fig. 2E, which confirms that the TA exosome is a supplier of TA antigens. However, the BRD2 protein of 110 kDa was not detected in the exosomal fraction of HepG2 cells using XC246 or a commercial anti-BRD2 antibody. Instead of the full-sized BRD2 form, the XC246 antibody detected a protein band of ~65 kDa (Fig. 2E), whereas the commercial anti-BRD2 antibody did not detect it. The immunogen of the commercial anti-BRD2 antibody has been reported as the 179-259 amino acids of BRD2. Epitope mapping analysis using a series of truncated recombinant BRD2 proteins revealed that the commercial anti-BRD2 antibody recognized the region between residues 179 and 205 of BRD2. It also revealed that the XC246 autoantibody recognized the region between residues 206 and 229 of BRD2 (Fig. S6). Based on these results, it was

Table I. Mass spectrometric analysis of XC246 antigen.

Accession number	Identified proteins	Molecular mass (Da)	pI	% mol[a]/score[b]	
				Band-1	Band-2
P13639	EEF2	96,246	6.41	0.9864/555	4.002/1645
P49588	AARS	107,484	5.34	0.9059/771	2.906/1883
A0A140T9E9	BRD2	88,664	9.13	-	2.7652/1357
Q14697-2	GANAB	109,825	5.82	-	1.6993/934
P53618	COPB1	108,214	5.72	0.9461/603	1.6692/779
K7EJE8	LONP1	93,637	6.08	-	1.6692/848
P22314	UBA1	118,858	5.49	0.2416/274	1.3876/1532
P34932	HSPA4	95,127	5.11	0.4328/397	1.3273/789
Q7KZF4	SND1	102,618	6.74	0.3624/328	1.3172/1019
E9PLK3	NPEPPS	103,720	5.41	0.8455/450	1.2971/734
P55060	CSE1L	111,145	5.51	0.4731/313	1.2267/709
O00159-3	MYO1C	120,352	9.5	0.3624/307	1.1966/1007
Q9Y678	COPG1	98,967	5.32	0.4127/185	1.1262/683
P33991	MCM4	97,068	6.28	0.6543/273	1.0357/558
P19367	HK1	103,561	6.36	0.0906/65	1.0055/579

Protein identification was performed using ESI-TRAP mass spectrometry; Mascot version 2.4.1; Database: UniProt_proteome_hu; total sequences, 93,614; total residues, 370,398,36; sequences after taxonomy filter, 93614; number of queries/matches, 9,144/1,540 (band-1), 11,146/1,014 (band-2), 8,877/1,224 (band-3), 9,664/1,304 (band-4). [a]% mol, expressed in moles unit of the amount of a constituent divided by the total amount of all constituents with a denominator of 100 in a mixture. [b]Score: the score is a statistical score calculated using Mascot software for how well the experimental data match the database sequence. EEF2, elongation factor 2; AARS, alanine-tRNA ligase; BRD2, bromodomain-containing protein 2; GANAB, isoform 2 of Neutral alpha-glucosidase AB; COPB1, coatomer subunit beta; LONP1, lon protease homolog; UBA1, ubiquitin-like modifier-activating enzyme 1; HSPA4, heat shock 70 kDa protein 4; SND1, staphylococcal nuclease domain-containing protein 1; NPEPPS, aminopeptidase; CSE1L, exportin-2; MYO1C, isoform 3 of Unconventional myosin-Ic; COPG1, coatomer subunit gamma-1; MCM4, DNA replication licensing factor; HK1, hexokinase-1.

concluded that the exosomal BRD2, a truncated BRD2 with a molecular weight of about 65 kDa and containing 206-229 amino acid residues of BRD2, is a post-translationally modified form of BRD2 that confers a neo-epitope for generating autoantibodies.

Epitope mimicry against the XC246 antibody screened from a phage-display random cyclic heptapeptide library can be used as antigenic determinants to detect TA autoantibodies instead of the cellular BRD2 antigen. While epitope mapping of XC246 antibody was performed by using recombinant BRD2 proteins and western blot analysis, these recombinant proteins are not appropriate for the detection of serum autoantibody using ELISA, due to their relatively low affinity to the antibody, as demonstrated in a previous study by the authors (16). In addition, some post-translational modifications that confer neo-epitopes for generating autoantibodies were anticipated. Therefore, high-affinity mimotopes were screened, which are the mimics of the conformational antigenic determinants, from a random cyclic peptide CX_7C library, as described in previous studies (16-18,32,33).

The biopanning of the M13 phage library containing 10^{11} cyclic peptides was repeated four rounds with the XC246 autoantibody, consequently enriching the cyclic peptide display M13 phages specific to the XC246 antibody (Fig. 3A). The cyclic peptide sequences displayed on selected phages were determined by sequencing 20 selected M13 phage clones, and 10 different epitopes were confirmed (Table II). These phages displayed high reactivity only to the XC246 autoantibody in ELISA, not to other TA autoantibodies, i.e., K94 (32) or XC90 (17) (Fig. 3B). Among the selected peptide epitopes,

Table II. Epitope peptide sequences (C-X7-C*) of selected phages against XC246 autoantibody.

Phage antigen	Phage epitope sequence (-$\underline{C}X_7\underline{C}$*-)
XC246p1	C-SSMFLPS-C
XC246p2	C-SSQWLPF-C
XC246p3	C-TSALFPW-C
XC246p4	C-VSASFPF-C
XC246p5	C-NQVAYPW-C
XC246p6	C-FSALYPW-C
XC246p7	C-CRLRWPH-C
XC246p8	C-TSSFFPH-C
XC246p9	C-TSVFLPH-C
XC246p10	C-STAMALV-C

C, cysteine residues forming disulfide bond of cyclic peptide epitope; X, all amino acids except cysteine.

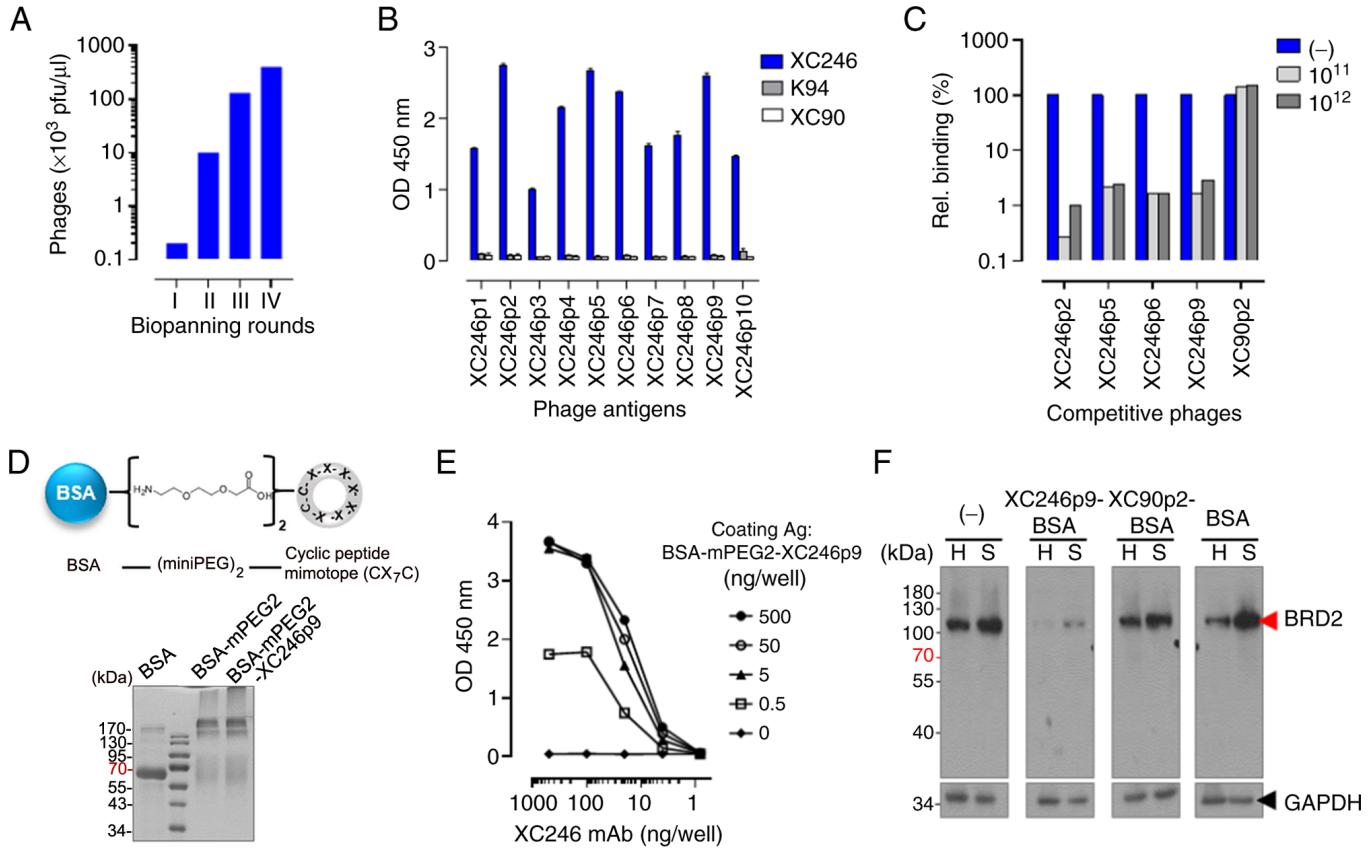

Figure 3. BRD2 autoantibody ELISA was developed using XC246p9 epitope-conjugated BSA for the detection of autoantibodies in human sera. (A) Biopanning of a phage-display random cyclic heptapeptide library for the isolation of epitope mimicries of the XC246 antigen. (B) Phage ELISA to confirm the binding specificity of the selected epitope mimicry phages to the XC246 autoantibody. M13 phages were coated with 10^{11} pfu phages per well. Primary antibodies were used at the concentration of 0.1 μg/well. Unrelated autoantibodies [K94 (32) and XC90 (17)] were used as non-related controls. (C) Competitive FACS analysis of XC246 autoantibody binding to XC246 phages or HepG2 cells. Fixed and permeabilized cells ($1x10^5$ cells/reaction) were treated with the XC246 autoantibody (0.5 μg). For antibody binding competition with the selected phages, cells were treated with the XC246 antibody pre-incubated with each phage (10^{11} or 10^{12} pfu/reaction), as indicated. (D) Preparation of the BSA-miniPEG2-XC246p9 antigen. A cyclic peptide with two miniPEG spacers, miniPEG2-XC246p9, was chemically synthetized and conjugated to bovine serum albumin (BSA) via amine-carboxyl acid coupling using the EDC reagent. The peptide-BSA conjugates (5 μg/lane) were analyzed by SDS-PAGE and Coomassie blue staining. BSA-miniPEG2 without the epitope peptide was prepared as a control antigen. The synthetic peptide-conjugated to BSA was observed as a high-molecular-weight protein band. (E) ELISA with the BSA-miniPEG2-XC246p9 antigen. The antigen was coated at the indicated amount and detected with a gradually diluted XC246 autoantibody. (F) Competitive western blot analysis of XC246 autoantibody binding to the BSA-miniPEG2-XC246p9 antigen or tumor cell lysates. The cell lysates [HepG2 (H) or SNU638(S)] were loaded at a quantity of 15 μg per lane, and BRD2 was detected with the XC246 autoantibody (1 μg/ 10 ml). For the competitive inhibition of antibody binding to cell lysates, the XC246 antibody was pre-incubated with the BSA-miniPEG2-XC246p9 antigen (0.6 μg/ml). BSA-miniPEG2-XC90p2 or BSA was used as the control competitor. The XC90p2 sequence is as follows: CPVRSGFPC. GAPDH was used as a loading control. BRD2, bromodomain-containing protein 2; BSA, bovine serum albumin.

the XC246p2, XC246p5, XC246p6, and XC246p9 sequences showed high reactivity to the XC246 autoantibody (Fig. 3B, Table II). The XC246 antibody-specific epitopes had the consensus sequence of $C\text{-}_XS_{XX}LP_X\text{-}C$ (Table II). XC246-specific phages competitively blocked XC246 antibody binding to HepG2 cells, as demonstrated by FACS analysis (Fig. 3C), indicating that the selected cyclic peptide with high affinity to the XC246 autoantibody can mimic the specific epitope on the cellular antigen BRD2. However, linearization of the cyclic peptide by treatment with a reducing agent resulted in the loss of those antigenic properties (Fig. S7), indicating that the conformational properties of the mimotope are critical for antibody binding.

To construct an ELISA for the detection of serum BRD2 autoantibodies, a sufficient supply of target antigen is needed. Epitope-display M13 phages can be used as coating antigens, as described in previous studies (32,33); however, phage amplification and purification are cumbersome processes. Therefore, synthetic cyclic peptide-conjugated BSA was prepared and used as a coating antigen to display the autoantigen-mimic epitope peptides. For the synthesis of epitope peptide, the XC246p9 sequence was selected (Table II), which does not contain less stable amino acids than others, including Q, M, W, N and D, which are prone to side reactions. Peptide epitope was cyclized by disulfide bonding between the two cysteine residues located at the N- terminus and C- terminus of the 9-mer peptide. Two miniPEG were conjugated to the N- terminus of the peptide as a spacer, and miniPEG2-linked cyclic peptides were conjugated to BSA via the EDC reaction (Fig. 3D). MiniPEG2-conjugated BSA without a peptide epitope was also prepared and used as a control antigen (Fig. S8). BSA-miniPEG2-XC246p9 demonstrated high affinity to the XC246 autoantibody, as shown using ELISA (Figs. 3E). BSA-miniPEG2-XC246p9 also blocked the binding of the

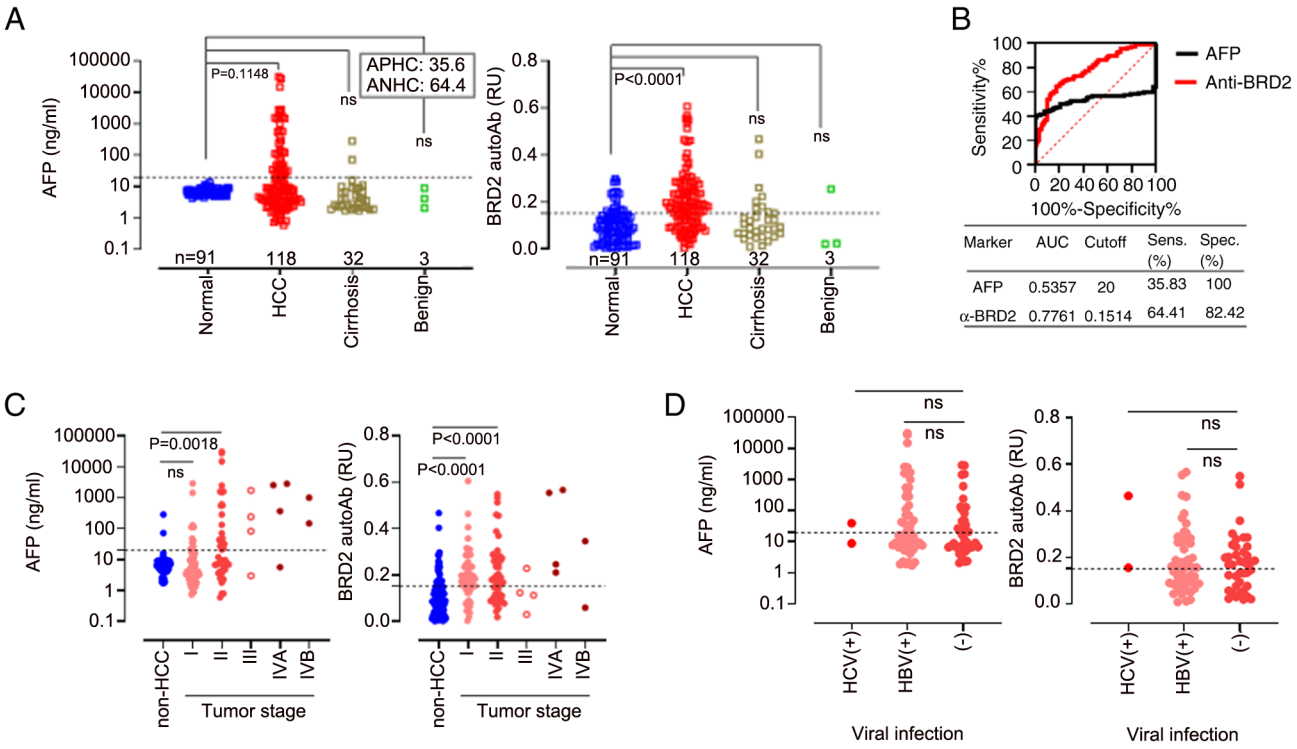

Figure 4. Human serum BRD2 autoantibody ELISA using BSA-miniPEG2-XC246p9 differentiated patients with HCC from non-HCC subjects. (A) AFP test and BRD2 autoantibody ELISA using BSA-miniPEG2-XC246p9 in sera of patients with HCC, as well as non-tumor subjects. The sample distribution was as follows: Control (n=91), HCC (n=118), cirrhosis (n=32) and benign liver cancer (n=3). Serum AFP levels were measured using a commercial quantification kit. The CV of AFP was 20 ng/ml, and the proportion of AFP-positive or -negative HCC (APHC or ANHC) is indicated within the box. The specific binding of the serum autoantibody to the XC246p9 epitope (anti-BRD2 response) was described as the difference in OD between the ELISA with BSA-miniPEG2-XC246p9 and that with BSA-miniPEG2. (B) The ROC curve analysis revealed the diagnostic sensitivity and specificity of each biomarker. All experiments were performed in duplicate and repeated at least three times. (C) Serum AFP and BRD2 autoantibody response related to tumor stage. The non-HCC group included control, cirrhosis, and benign liver cancer samples. (D) Serum AFP and BRD2 autoantibody response related to viral infection. The clinicopathological features of the participants are described in detail in Table III. ns, not significant (P>0.05); BRD2, bromodomain-containing protein 2; BSA, bovine serum albumin; HCC, hepatocellular cancer; CV, cut-off value; APHC, AFP-positive HCC; ANHC, AFP-negative HCC; AFP, serum alpha-fetoprotein.

XC246 autoantibody to the endogenous antigen in tumor cells (HepG2 or SNU638), as revealed by competitive western blot analysis (Fig. 3F).

Collectively, the TA autoantibody XC246, which was generated in the HCC model mouse via an autoimmune response to the TA antigen BRD2, reacted with the XC246p9 cyclic peptide epitope with high affinity, and XC246p9 peptide-conjugated BSA was prepared for the detection of the BRD2 autoantibody in human serum.

Human serum ELISA using the BSA-conjugated BRD2-mimic epitope can differentiate patients with HCC from control subjects. Human serum ELISA for the BRD2 autoantibody biomarker was performed using XC246p9 peptide-conjugated BSA under conditions optimized for each step as follows: BSA-mini-PEG2-XC246p9 was employed as a coating antigen in ELISA using a Maxisorp plate. BSA-mini-PEG2 was also used as a negative control antigen. For blocking non-specific reactions of human sera to the antigen-coated plates, the plates were treated with a blocking buffer containing PVP, Ficoll and PFBB, as described in the 'Materials and methods'. Human serum samples were heat-inactivated at 50˚C for 5 min and diluted 50-fold in blocking buffer. The sera of 118 patients with HCC and 91 healthy controls were analyzed for the BRD2 autoantibody biomarker. The patients' sera with cirrhosis (n=32) and benign cancer (n=3) were also analyzed. The level of BRD2 autoantibody biomarker was determined as the difference in OD between the ELISA for BSA-mini-PEG2-XC246p9 and that for BSA-mini-PEG2. As demonstrated in Fig. 4A, the BRD2 autoantibody biomarker was significantly elevated in the sera of patients with HCC compared with healthy subjects. The sensitivity of ELISA was 64.41% and the specificity 82.42% for the cut-off value of 0.1514, with an AUC value of 0.7761 [95% CI: 0.7136-0.8386, P<0.0001] (Fig. 4B).

AFP levels, a most widely used HCC biomarker, were also analyzed in the same HCC cohort. All healthy controls had a serum AFP levels below the cut-off value of 20 ng/ml (Fig. 4A). However, not all patients with HCC had a serum AFP level above the cut-off value. AFP levels >20 ng/ml were detected only in 35.6% (42/118) of the patients with HCC and in 6.25% (2/32) of those with cirrhosis. A ROC curve analysis for the serum AFP test yielded an AUC value of 0.5357 [95% CI, 0.4514-0.6200; P=0.3746]. The sensitivity was 35.83%, and the specificity was 100% for the cut-off value of 20 ng/ml AFP (Fig. 4B).

The detection patterns of these markers were dependent on the tumor stage. The AFP levels progressively increased in patients with HCC as the tumor stage advanced (Fig. 4C). However, BRD2 autoantibody levels were significantly high

Table III. The clinicopathological features of the validation cohort[a].

Parameters	Patients, n (%)	BRD2 autoantibody[b]		ATIC autoantibody[c]	
		<CV, n (%)	≥CV, n (%)	<CV, n (%)	≥CV, n (%)
All cases	120 (100.0)	63 (52.5)	57 (47.5)	54 (45.0)	66 (55.0)
Age distribution (years) 33-83					
<55	37 (30.8)	21 (17.5)	16 (13.3)	18 (15.0)	19 (15.8)
≥55	83 (69.2)	42 (35.0)	41 (34.2)	36 (30.0)	47 (39.2)
Sex					
Male	104 (86.7)	56 (46.7)	48 (40.0)	48 (40.0)	56 (46.7)
Female	16 (13.3)	7 (5.8)	9 (7.5)	6 (5.0)	10 (8.3)
Viral infection					
HBV	39 (32.5)	26 (21.7)	13 (10.8)	25 (20.8)	14 (11.7)
HCV	2 (1.7)	0 (0.0)	2 (1.7)	0 (0.0)	2 (1.7)
No infection	79 (65.8)	37 (30.8)	42 (35.0)	29 (24.2)	50 (41.7)
TNM stage[d]					
I	60 (50.0)	24 (20.0)	36 (30.0)	22 (18.3)	38 (31.7)
II	50 (41.7)	32 (26.7)	18 (15.0)	26 (21.7)	24 (20.0)
III	4 (3.3)	3 (2.5)	1 (0.8)	2 (1.7)	2 (1.7)
IVA+AB	6 (5.0)	4 (3.3)	2 (1.7)	4 (3.3)	2 (1.7)
Serum AFP concentration: 0.8-83000 ng/ml					
<20 ng/ml	77 (64.2)	41 (34.2)	36 (30.0)	34 (28.3)	43 (35.8)
≥20 ng/ml	43 (35.8)	22 (18.3)	21 (17.5)	20 (16.7)	23 (19.2)

[a]HCC serum samples were provided by National Biobank of Korea (Ajou Human Bio-Resource Bank). [b]CV for serum BRD2 autoantibody is 0.1514, and the significance values derived from statistical analysis of this data are described in Fig. 4B. [c]CV for serum ATIC autoantibody is 0.6125, and the significance values derived from statistical analysis of this data are described in Fig. S9A. [d]TNM stage of patients with HCC was classified according to the modified UICC system (38,39). HCC, hepatocellular cancer; BRD2, bromodomain-containing protein 2; AFP, serum alpha-fetoprotein; ATIC, AICAR transformylase/inosine monophosphate cyclohydrolase; CV, cut-off value; HBV, hepatitis B virus; HCV, hepatitis C virus; TNM, tumor-node-metastasis; AFP, alpha-fetoprotein; UICC, Union for International Cancer Control.

even in tumor stage I (P≤0.0001), maintaining those levels throughout all tumor stages (Fig. 4C). The presence or absence of viral infection in patients with HCC was not associated with these two markers in this cohort (Fig. 4D).

The simultaneous detection of AFP and BRD2 autoantibody in patient sera improves the accuracy of the HCC diagnosis. AFP is a typical protein biomarker of HCC that is secreted into the blood via a signal peptide from liver tissue. By contrast, TA autoantibody biomarkers appeared to be induced by TA antigens, that are released as components of the tumor exosome. The release mechanism of the tumor exosome is different from that of secretory proteins, which may reflect other aspects of tumor characteristics. The correlation between the anti-BRD2 response and AFP was analyzed using Pearson's correlation analysis, expecting that AFP and TA autoantibody biomarkers would represent different characteristics of tumors. The correlation between the BRD2 autoantibody and AFP in sera was very low (Fig. 5A left panel; Pearson's coefficient, r=0.04240; P=0.5097), suggesting that the appearance of these two serum markers is regulated by unrelated mechanisms. However, the BRD2 autoantibody responses in patients with HCC were highly correlated with another HCC autoantibody biomarker, the ATIC autoantibody (Fig. 5A right panel; Pearson's coefficient, r=0.7749; P<0.0001). The ATIC autoantibody (16) was detected in the same cohort, using the BSA-miniPEG2-XC154p1 antigen which was prepared according to the procedures used for the generation of the BSA-conjugated XC246p9 antigen. This biomarker was observed to be significantly elevated in the serum of patients with HCC as compared with that of healthy subjects (Fig. S9A), with an AUC value of 0.8262 [Fig. S9B; 95% CI, 0.7700-0.8824, P<0.0001]. The sensitivity of the ELISA for ATIC autoantibody was 64.41%, and the specificity was 78.02% for the cut-off value of 0.6125 (Fig. S9B). The correlation between the ATIC autoantibody and the BRD2 autoantibody detection in sera was strong (Pearson's coefficient, r=0.7749; P<0.0001), although their responses were not identical (Fig. 5A). Pearson's correlation analysis also was performed on the individual cohorts. As shown in Fig. S10, the AFP and anti-BRD2 autoantibody biomarker pairs exhibited correlation coefficients of -0.025, 0.105, 0.217 and -0.226 in the HCC, normal, cirrhosis and benign cohorts, respectively, indicating that there was no significant correlation between the two biomarkers in all cohorts. By contrast, the autoantibody biomarker pair (anti-BRD2 and anti-ATIC) demonstrated positive correlation coefficients (0.795, 0.602, 0.706, and 0.460) in all cohorts, confirming the correlation between autoantibody biomarkers.

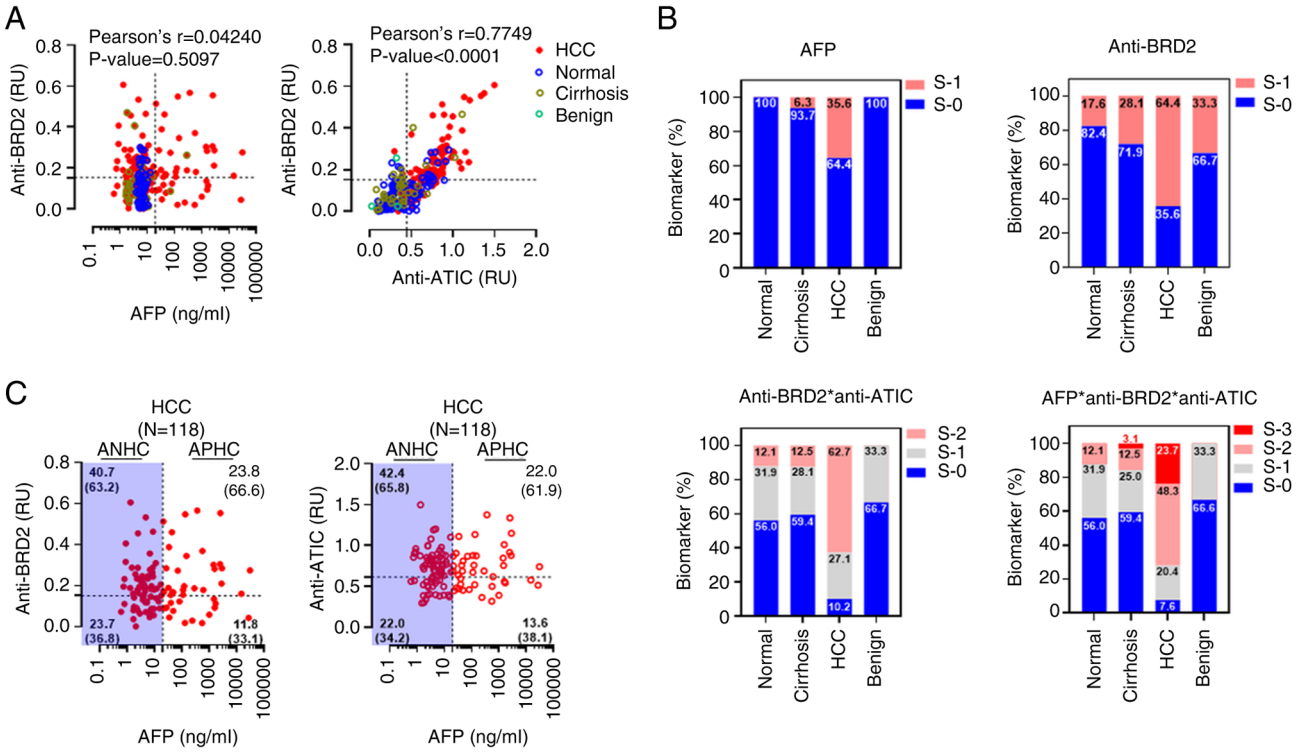

Figure 5. Combined analysis of serum autoantibody biomarkers with AFP enhanced the diagnostic accuracy of HCC. (A) Pearson's analysis of the correlations between the BRD2 autoantibody biomarker and the AFP or ATIC autoantibodies. The dotted lines represent the cutoff value of each biomarker diagnosis. The results of Pearson's analysis in individual cohorts are depicted in Fig S10. (B) Combined analysis of HCC biomarkers, AFP, BRD2 autoantibody, or ATIC autoantibody. The diagnostic values of each biomarker shown in panel A (AFP, anti-BRD2, and anti-ATIC) were simplified as either S-1 or S-0 according to whether their detection values surpassed or fail the cut-off value. Subsequently, the diagnostic values of each biomarker or their combination were analyzed. For the combined analysis of these markers, the unified diagnostic indexes of a serum sample were simply added and designated triple-negative samples as S-0, single-positive samples as S-1, double-positive samples as S-2, and triple-positive samples as S-3. The numbers on the plots represent the percentage of corresponding subjects. (C) Scattered plot analysis of HCC biomarker responses depending on AFP and autoantibody biomarker. The numbers in each quadrant represent the percentage of each case among patients with HCC (n=118). The numbers in the parentheses are the proportion of autoantibody biomarker-positive or -negative samples among ANHC or APHC cases. HCC, hepatocellular cancer; BRD2, bromodomain-containing protein 2; AFP, serum alpha-fetoprotein; ATIC, AICAR transformylase/inosine monophosphate cyclohydrolase; S-1, responsive; S-0, non-responsive; S-2, double positive; S-3, triple positive; ANHC, AFP-negative HCC; APHC, AFP-positive HCC.

The simultaneous detection of cancer biomarkers representing the different properties of cancer would enhance diagnostic accuracy. To examine the effects of the combined analysis of BRD2 or ATIC autoantibody biomarker and AFP, the response of each biomarker was simplified to positive or negative and scored as 1 or 0, depending on whether the detection value was higher or lower than the cutoff value. The combined analysis of these biomarkers was performed by the simple addition of each score, which resulted in values of 0, 1, 2, or 3 (Fig. 5B). The proportion of AFP-positive patients with HCC in the present cohort was 35.6%, and the percentage of BRD2 autoantibody-positive patients with HCC was 64.4%. The simultaneous detection of the two autoantibody biomarkers (anti-BRD2 and anti-ATIC) increased the proportion of biomarker-positive HCC patients (score 1 and 2) to 89.8%. In addition, the combined detection of AFP and two TA autoantibody biomarkers (score 1, 2 and 3) could be detected in up to 92.4% of the patients with HCC. However, a notable proportion of autoantibody-biomarker-positive cases (score 1 and 2) was also observed among the normal healthy participant cohort (44.0%).

The diagnosis of HCC is straightforward when significantly increased serum AFP levels and definitive imaging features are present. However, AFP-negative hepatic cancer (ANHC) is not as easily diagnosed, as the majority of ANHCs are early and small HCCs, often without typical imaging characteristics (34). The diagnosis of ANHC is crucial in clinical practice, because ANHC accounts for nearly half of HCC cases and has a better prognosis compared to AFP-positive HCC (APHC). The BRD2 autoantibody biomarker was analyzed in patients with ANHC or APHC from the present HCC cohort (Fig. 5C). In the APHC group, 66.6% of the patients with HCC exhibited a positive BRD2 autoantibody biomarker response. The BRD2 autoantibody biomarker was also detected as positive in 63.2% of ANHC cases. The ATIC autoantibody response in APHC or ANHC cases was similar to that of the BRD2 autoantibody. However, ~20% of all patients with HCC were determined to be double-negative for these biomarkers (Fig. 5C).

Discussion

Patients with HCC are known to be frequently asymptomatic, and the appearance of symptoms can signal the development of severe disease. Therefore, the early diagnosis of HCC followed by effective treatment is currently critical for improving the prognosis and reducing the associated economic burden (34). AFP is by far the most widely used serum HCC biomarker.

However, its sensitivity for HCC diagnosis is only 41-65% with a specificity of 80-94% (34).

The present study demonstrated that the anti-BRD2 response can be used to diagnose liver cancer that is not be screened by AFP (Fig. 5C). In the cohort used in the present study, AFP was detected only in 35.6% of the patients with HCC, whereas the BRD2 autoantibody was present in 64.4% of the patients with HCC. Among the AFP-positive patients with HCC, 66.6% were positive for the BRD2 autoantibody and 63.2% of the AFP-negative patients with HCC were also positive for the BRD2 autoantibody biomarker. Non-responders to AFP, as well as the anti-BRD2 antibody biomarker comprised the remaining 23.7% of the patients with HCC. However, the fraction of non-responders to the HCC biomarkers was decreased to 7.6% by additional detection with the ATIC autoantibody (Fig. 5B). TA autoantibodies are biologically amplified signals, corresponding to TA antigens and hence may be measurable early on, designating them as promising early biomarkers. However, the antibody response to each antigen depends on the individual's immune system, and the amount of antibody will not be exactly proportional to the amount of antigen. Therefore, in cancer diagnosis using autoantibody biomarkers, it is necessary to concurrently measure various autoantibodies in order to increase accuracy (11,12). The majority of autoantibody cancer biomarker studies intend to propose a multiple diagnostic autoantibody panel (11,12). From the results of the present study, it can also be confirmed that the diagnostic efficiency is improved by simultaneously measuring two autoantibodies and AFP and the potential of multiplex detection of autoantibody biomarkers with AFP as a liver cancer diagnosis.

Additional verification is required of whether TA autoantibodies are detected even in in individuals classified as normal without HCC. In the present study, the corresponding individuals appeared to be exposed to abnormal antigens released from tissues, which induce antigen-specific autoantibodies, although their association with HCC is not evidenced. Autoantibody detection in normal subjects can be an important signal predicting inflammations or liver diseases. Follow-up of the serum donor may be required to confirm the disease-related characteristics of the serum donor.

TA autoantigens, which confer neo-epitopes to the immune system, can be oncogenic drivers or support tumorigenesis. The overexpression of the TA antigen ATIC (16) can function as an oncogenic gene that promotes survival, proliferation, and migration by targeting AMPK-mTOR-S6 K1 signaling (35). The genetic deletion of fatty acid synthase (FASN), which is another TA antigen (33), suppresses the hepatocarcinogenesis driven by AKT and AKT/c-Met proto-oncogenes in mice (36), which implicates the crucial role of FASN during tumorigenesis. The abundance of BRD2, as well as its high genetic alternation rate (~19%) in patients with HCC have been shown to be associated with a worse overall survival (37). However, the oncogenic properties of upregulated BRD2 in liver cancer have not been directly confirmed, which can be examined in further studies.

Although the characteristics of the neo-epitope that induce BRD2 autoantibody, including genetic alteration, post-translational modification, abundance, or localization, were not defined in detail in the present study, evidence was provided, suggesting the presence of a neo-epitope on oncogenic BRD2. The BRD2 autoantibody obtained from the HCC mouse model, XC246, exhibited an unexpected pattern of intracellular staining for BRD2 in tumor cells. In contrast to the commercial anti-BRD2 antibody, which stains BRD2 mainly in the nucleus, the BRD2 autoantibody, XC246, stained the cytoplasmic BRD2. Furthermore, the XC246 antibody detected the exosomal BRD2, which was not detected using the commercial antibody. It is anticipated that these characteristics of BRD2 are related to the neo-epitope, which generates the autoantibody.

To develop a detection method for the serum BRD2 autoantibody, the structural features of the neo-epitope must be reflected in the capture antigen used in ELISA. Therefore, the epitope mimicries from a conformational peptide library were screened, using the BRD2 autoantibody, and then applying it as an antigen in serum TA autoantibody ELISA, instead of the recombinant BRD2 protein. It has been previously demonstrated that cyclic peptide epitopes fused to streptavidin are sufficient to capture serum autoantibodies (16-18). In the present study, a synthetic cyclic peptide epitope-conjugated antigen was prepared, in order to simplify the preparation process of the coating antigen. In addition, BSA was used as a carrier protein to reduce non-specific binding in the human serum ELISA. Synthetic cyclic peptide epitopes fully mimicked the cellular antigenic property, as revealed by ELISA and competitive western blotting and were proven to be appropriate for serum ELISA. The ATIC autoantibody was also detected using peptide epitope-conjugated BSA instead of the streptavidin conjugate used in a previous study (16). These results demonstrated that BSA-conjugated mimotope peptides are sufficient for detecting specific autoantibodies, offering the possibility of its application to the detection of other autoantigenic epitope mimics (16-18,32,33).

In conclusion, the present study suggested that the BRD2 autoantibody can be used as an HCC-associated biomarker and the feasibility of serum BRD2 autoantibody ELISA using a specific conformational epitope against the BRD2 autoantibody. Serum BRD2 autoantibody ELISA was also proposed as an accompanying test to serum AFP detection for the enhancement of HCC diagnostic efficiency. Further studies on the serum BRD2 autoantibody using large and well-defined cohorts are necessary to corroborate its usefulness for cancer diagnosis.

Acknowledgements

Not applicable.

Funding

The present study was supported by the Korea Research Institute of Bioscience and Biotechnology Research Initiative Program (grant no. KGM9942213) and the National Research Foundation of Korea grant (grant no. NRF-2020R1A2C2014433) funded by the Ministry of Science and ICT of Korea.

Availability of data and materials

The datasets used and/or analyzed during the current study are available from the corresponding author on reasonable request.

Author's contributions

CKH, WHL and EWC designed the experiments. CKH, WHL, IP and YSC performed the experiments and collected the data. CKH, WHL, YSC, KJL and EWC analyzed and interpreted the data. CKH, WHL and EWC drafted the manuscript. CKH and EWC revised the manuscript critically. CKH, WHL and YSC confirm the authenticity of all the raw data. All the authors have read and approved the final manuscript.

Ethics approval and consent to participate

The Public Institutional Review Board of the Ministry of Health and Welfare reviewed the contents of the present study and confirmed that research using commercialized human tissue falls under the exemption categories specified by Bioethics and Safety Act in Korea (IRB No. P01-202008-31-009; Republic of Korea). The study followed the ethical guidance of Ministry of Health and Welfare in Republic of Korea.

Patient consent for publication

Not applicable.

Competing interests

The authors declare that they have no competing interests.

References

1. World Health Organization (WHO): Cancer. WHO, Geneva, 2022. https://www.who.int/news-room/fact-sheets/detail/cancer. Accessed February 3, 2022.
2. Philips CA, Rajesh S, Nair DC, Ahamed R, Abduljaleel JK and Augustine P: Hepatocellular carcinoma in 2021: An exhaustive update. Cureus 13: e19274, 2021.
3. Wong RJ, Cheung R and Ahmed A: Nonalcoholic steatohepatitis is the most rapidly growing indication for liver transplantation in patients with hepatocellular carcinoma in the U.S. Hepatology 59: 2188-2195, 2014.
4. Anstee QM, Reeves HL, Kotsiliti E, Govaere O and Heikenwalder M: From NASH to HCC: Current concepts and future challenges. Nat Rev Gastroenterol Hepatol 16: 411-428, 2019.
5. Forner A, Reig M and Bruix J: Hepatocellular carcinoma. Lancet 391: 1301-1314, 2018.
6. Hartke J, Johnson M and Ghabril M: The diagnosis and treatment of hepatocellular carcinoma. Semin Diagn Pathol 34: 153-159, 2017.
7. Marshall HT and Djamgoz MBA: Immuno-oncology: Emerging targets and combination therapies. Front Oncol 8: 315, 2018.
8. Vinay DS, Ryan EP, Pawelec G, Talib WH, Stagg J, Elkord E, Lichtor T, Decker WK, Whelan RL, Kumara HMCS, *et al*: Immune evasion in cancer: Mechanistic basis and therapeutic strategies. Semin Cancer Biol 35 (Suppl): S185-S198, 2015.
9. Sharonov GV, Serebrovskaya EO, Yuzhakova DV, Britanova OV and Chudakov DM: B cells, plasma cells and antibody repertoires in the tumour microenvironment. Nat Rev Immunol 20: 294-307, 2020.
10. Macdonald IK, Parsy-Kowalska CB and Chapman CJ: Autoantibodies: Opportunities for early cancer detection. Trends Cancer 3: 198-213, 2017.
11. Kobayashi M, Katayama H, Fahrmann JF and Hanash SM: Development of autoantibody signatures for common cancers. Semin Immunol 47: 101388, 2020.
12. de Jonge H, Iamele L, Maggi M, Pessino G and Scotti C: Anti-cancer auto-antibodies: Roles, applications and open issues. Cancers (Basel) 13: 813, 2021.
13. Sexauer D, Gray E and Zaenker P: Tumour-associated autoantibodies as prognostic cancer biomarkers-a review. Autoimmun Rev 21: 103041, 2022.
14. Wouters MCA and Nelson BH: Prognostic significance of tumor-infiltrating B cells and plasma cells in human cancer. Clin Cancer Res 24: 6125-6135, 2018.
15. Zheng M, Li YM, Liu ZY, Zhang X, Zhou Y, Jiang JL, Zhu P, Yang XM, Tang J and Chen ZN: Prognostic landscape of tumor-infiltrating T and B cells in human cancer. Front Immunol 12: 731329, 2022.
16. Heo CK, Hwang HM, Lim WH, Lee HJ, Yoo JS, Lim KJ and Cho EW: Cyclic peptide mimotopes for the detection of serum Anti-ATIC autoantibody biomarker in hepato-cellular carcinoma. Int J Mol Sci 21: 9718, 2020.
17. Heo CK, Hwang HM, Lee HJ, Kwak SS, Yoo JS, Yu DY, Lim KJ, Lee S and Cho EW: Serum anti-EIF3A autoantibody as a potential diagnostic marker for hepatocellular carcinoma. Sci Rep 9: 11059, 2019.
18. Hwang HM, Heo CK, Lee HJ, Kwak SS, Lim WH, Yoo JS, Yu DY, Lim KJ, Kim JY and Cho EW: Identification of anti-SF3B1 autoantibody as a diagnostic marker in patients with hepatocellular carcinoma. J Transl Med 16: 177, 2018.
19. Zhang XD, Wang Y and Ye LH: Hepatitis B virus X protein accelerates the development of hepatoma. Cancer Biol Med 11: 182-190, 2014.
20. Hsieh A, Kim HS, Lim SO, Yu DY and Jung G: Hepatitis B viral X protein interacts with tumor suppressor adenomatous polyposis coli to activate Wnt/β-catenin signaling. Cancer Lett 300: 162-172, 2011.
21. Yu DY, Moon HB, Son JK, Jeong S, Yu SL, Yoon H, Han YM, Lee CS, Park JS, Lee CH, *et al*: Incidence of hepatocellular carcinoma in transgenic mice expressing the hepatitis B virus X-protein. J Hepatol 31: 123-132, 1999.
22. National Library of Medicine (NIH): BRD2 bromodomain containing 2. NIH, Bethesda, MD, 2022. https://www.ncbi.nlm.nih. gov/gtr/genes/6046/. Updated October 9, 2022.
23. Loganathan SN, Tang N, Fleming JT, Ma Y, Guo Y, Borinstein SC, Chiang C and Wang J: BET bromodomain inhibitors suppress EWS-FLI1-dependent transcription and the IGF1 autocrine mechanism in Ewing sarcoma. Oncotarget 7: 43504-43517, 2016.
24. Sun LY, Spong A, Swindell WR, Fang Y, Hill C, Huber JA, Boehm JD, Westbrook R, Salvatori R and Bartke A: Growth hormone-releasing hormone disruption extends lifespan and regulates response to caloric restriction in mice. Elife 2: e01098, 2013.
25. Belkina AC, Blanton WP, Nikolajczyk BS and Denis GV: The double bromodomain protein Brd2 promotes B cell expansion and mitogenesis. J Leukoc Biol 95: 451-460, 2014.
26. Pathak S, Stewart WCL, Burd CE, Hester ME and Greenberg DA: Brd2 haploinsufficiency extends lifespan and healthspan in C57B6/J mice. PLoS One 15: e0234910, 2020.
27. Hnilicova J, Hozeifi S, Stejskalova E, Duskova E, Poser I, Humpolickova J, Hof M and Staněk D: The C-terminal domain of Brd2 is important for chromatin interaction and regulation of transcription and alternative splicing. Mol Biol Cell 24: 3557-3568, 2013.
28. Suppiah A and Greenman J: Clinical utility of anti-p53 autoantibody: Systematic review and focus on colorectal cancer. World J Gastroenterol 19: 4651-4670, 2013.
29. Zaenker P, Gray ES and Ziman MR: Autoantibody production in cancer-the humoral immune response toward autologous antigens in cancer patients. Autoimmun Rev 15: 477-483, 2016.
30. Kato T, Fahrmann JF, Hanash SM and Vykoukal J: Extracellular vesicles mediate B cell immune response and are a potential target for cancer therapy. Cells 9: 1518, 2020.
31. Hao Q, Wu Y, Wu Y, Wang P and Vadgama JV: Tumor-derived exosomes in tumor-induced immune suppression. Int J Mol Sci 23: 1461, 2022.
32. Heo CK, Hwang HM, Ruem A, Yu DY, Lee JY, Yoo JS, Kim IG, Yoo HS, Oh S, Ko JH and Cho EW: Identification of a mimotope for circulating anti-cytokeratin 8/18 antibody and its usage for the diagnosis of breast cancer. Int J Oncol 42: 65-74, 2013.
33. Heo CK, Woo MK, Yu DY, Lee JY, Yoo JS, Yoo HS, Ko JH, Kim JM, Choi JY, Kim IG, *et al*: Identification of autoantibody against fatty acid synthase in hepatocellular carcinoma mouse model and its application to diagnosis of HCC. Int J Oncol 36: 1453-1459, 2010.
34. Wang T and Zhang KH: New blood biomarkers for the diagnosis of AFP-negative hepatocellular carcinoma. Front Oncol 10: 1316, 2020.

35. Li M, Jin C, Xu M, Zhou L, Li D and Yin Y: Bifunctional enzyme ATIC promotes propagation of hepatocellular carcinoma by regulating AMPK-mTOR-S6 K1 signaling. Cell Commun Signal 15: 52, 2017.
36. Che L, Pilo MG, Cigliano A, Latte G, Simile MM, Ribback S, Dombrowski F, Evert M, Chen X and Calvisi DF: Oncogene dependent requirement of fatty acid synthase in hepatocellular carcinoma. Cell Cycle 16: 499-507, 2017.
37. Chen YR, Ouyang SS, Chen YL, Li P, Xu HW and Zhu SL: BRD4/8/9 are prognostic biomarkers and associated with immune infiltrates in hepatocellular carcinoma. Aging (Albany NY) 12: 17541-17567, 2020.
38. Kudo M, Kitano M, Sakurai T and Nishida N: general rules for the clinical and pathological study of primary liver cancer, nationwide follow-up survey and clinical practice guidelines: The outstanding achievements of the liver cancer study group of Japan. Dig Dis 33: 765-770, 2015.
39. Korean Liver Cancer Study Group (KLCSG); National Cancer Center, Korea (NCC): 2014 Korean liver cancer study group-national cancer center Korea practice guideline for the management of hepatocellular carcinoma. Korean J Radiol 16: 465-522, 2015.